Cesium and iodine speciation in irradiated UO2 fuel

Colle, J. Y.; Zappey, J. N.; Beneš, O.; Cologna, M.; Wiss, T.; Konings, R. J.M.

DOI
10.1016/j.jnucmat.2025.155715

Publication date
2025

Document Version
Final published version

Published in
Journal of Nuclear Materials

Journal of Nuclear Materials 608 (2025) 155715

Contents lists available at ScienceDirect

Journal of Nuclear Materials

journal homepage: www.elsevier.com/locate/jnucmat

Cesium and iodine speciation in irradiated UO_2 fuel

J.-Y. Colle [a,*], J.N. Zappey [a,b], O. Beneš [a], M. Cologna [a], T. Wiss [a], R.J.M. Konings [a,b]

[a] European Commission, Joint Research Centre (JRC), Karlsruhe, Germany
[b] Delft University of Technology, Faculty of Applied Physics, Mekelweg 15, 2629 JB, Delft, the Netherlands

ARTICLE INFO

Keywords:
Nuclear fuel
Fission product release
Iodine
Cesium
Knudsen effusion mass spectrometry

ABSTRACT

The presence of CsI in nuclear fuel has long been debated. Its formation significantly decreases volatility, thereby reducing the rate at which iodine and cesium are released from the reactor core during a nuclear accident. A series of samples were investigated by Knudsen Effusion Mass Spectrometry (KEMS) in order to determine whether CsI is present in irradiated nuclear fuel. The examined samples were pure CsI, CsI exposed to gamma radiation, CsI-doped UO_2 simulated fuel and irradiated LWR fuel samples. The CsI and CsI-doped samples were examined to establish boundary conditions for the detection of CsI by KEMS. These samples indicated that the presence of CsI in fuel is characterized by three mass spectrometric signals Cs^+, I^+ and CsI^+, with a peak ratio of CsI^+ and I^+ of 1:0.7. The examinations of irradiated fuels showed none of these characteristics and hence no evidence that CsI is present in irradiated LWR nuclear fuel, at least after a storage period of years.

1. Introduction

The chemical state of the fission products in the matrix of a fuel pellet strongly depends on the oxygen potential (pO_2) and temperature (T) of the fuel [1–3]. The change in oxygen potential is governed by uranium fission. In stoichiometric fuel, tetravalent uranium binds two oxygen atoms. When uranium is split, the charge state of the newly created fission products is lower (< 4+) and they thus bind less oxygen than the original uranium atom. This results in excess oxygen that is incorporated in the UO_2 matrix by increasing the O/U ratio, resulting in an increase of the fuel's oxygen potential with fuel burn-up. The temperature change is also a result of uranium fission: it is determined by the fission power and the thermal conductivity of the fuel. The thermal conductivity of UO_2 is low, and deteriorates with burn-up [4], and hence a strong temperature profile occurs in fuel, from about 1500 K in the center to 650 K at the pellet rim [5].

Under influence of the local temperature and pO_2 the fission products take up a certain chemical speciation. They can remain in their elemental form or form compounds with other fission products or with oxygen or uranium from the matrix. Kleykamp [6] classified the fission products in four different groups: (1) the gases and volatiles (e.g. Xe, Kr, Cs and I) (2) the dissolved oxides (e.g. Ba, Mo, Sr and Cs) (3) ceramic inclusions (e.g. Nd, La, Mo and Cs) and (4) the metallic inclusions (e.g. Tc, Pd and Mo). As can be seen above, elements (e.g. Cs) can exist in different categories, and under influence of temperature and oxygen potential an element can make a transition from one group to another, making it inherently difficult to define their chemical state.

Knowing the chemical state of fission products in nuclear fuel is important as the speciation of fission products under normal conditions is directly related to the release of fission products under transient conditions. Two elements that are of particular interest are the fission products iodine and cesium. Both elements are volatile in their elemental form. However, when they would react to form cesium iodide [7], their volatility is drastically lowered and the probability of release from the reactor core is reduced.

Furthermore, Cs, I and CsI have different effects on the cladding of the fuel. In literature elemental iodine has been related to stress corrosion cracking of zircalloy cladding in LWR's (Light Water Reactor) [8–10], whereas CsI has been found not to have any effect on the zirconium cladding [8]. On the other hand Cs has been found to be corrosive for stainless steel cladding in fast reactors [11], whereas iodine has been found not to be corrosive [11,12].

It is often proposed that I is bonded to Cs in nuclear fuel [13–15]. Several arguments underpin this assumption. Firstly, cesium is produced in a ratio of 10 to 1 compared to iodine, which means that it is abundantly present in the fuel, enough for iodine to bind to. Secondly, CsI is a thermodynamically stable and energetically favorable compound under conditions found in nuclear reactors [16,17,1,18]. Thirdly, the irradiation periods are long - fuel resident times are up to four years - so reaction kinetics may play a minor role. Additionally, there is exper-

* Corresponding author.
E-mail address: jean-yves.colle@ec.europa.eu (J.-Y. Colle).

https://doi.org/10.1016/j.jnucmat.2025.155715
Received 17 June 2024; Received in revised form 3 February 2025; Accepted 25 February 2025

Available online 26 February 2025

imental evidence for this assumption. In a review of the speciation of iodine in nuclear fuel, Campbell et al. [19] concluded that "although discrepancies concerning the chemical form of iodine contained in and released from LWR fuel rods remain to be resolved, there appears to be little question that elemental iodine is not the dominant form in clad fuel. Instead, the dominant species is a considerably less volatile metal iodide; moreover, the experimental evidence strongly supports the thermodynamic calculations in indicating this metal iodide is CsI".

Collins et al. [20] presented experimental evidence pointing in the direction of the formation of CsI in nuclear fuel. They purged the pellet-cladding gap of fuel pins with helium at temperatures up to 1200 °C, collecting the volatile fraction. The purged fractions of iodine and cesium were essentially equal, leading to the conclusion that they originated from CsI. A second set of experiments conducted by Collins et al. was carried out in a steam-helium-hydrogen atmosphere with temperature ranging from 500 °C to 2000 °C. During these experiments only a small part of the iodine collected was in its elemental state that was able to penetrate the filter. The rest of the collected iodine in the test was characteristic for iodine originating from cesium iodide [20]. Note that Collins did not mention the time elapsed between the end of the irradiation and the release experiment. Another example is an experiment conducted by Davies et al. [21] that showed iodine does not travel into the plenum region, unlike the fission gases. This behavior was thought to be due to the formation of a metal iodide. More concrete evidence for the interaction of I and Cs was presented by Rochedy et al. [18], who concluded that CsI formed in UO_2 samples implanted with Cs and I atoms after thermal treatment at temperatures between 900 and 1200 °C, based on EDX, EELS and XANES analysis.

Besides evidence and arguments in favor of CsI formation in nuclear fuel there is also evidence indicating a limited stability. Cubiccioti et al. [22] studied the effect of gamma radiation on certain compounds, and found that in a strong radiation field reactions may not follow thermodynamic predictions. This is especially the case for metal iodides. They irradiated a capsule of CsI in a gamma pit to a dose of 10^7 Gy at a maximum temperature of 300 °C. Afterwards the capsule was placed in a mass spectrometer chamber at 0 °C and opened. The results showed that significant quantities of I_2 were released, from which they concluded that CsI dissociates in a gamma radiation field. It should be noted that at high temperature, typically temperatures that are reached during nuclear power production, Cs and I may recombine.

Additionally, Peehs et al. [23] conducted various experiments on both irradiated fuel and simulated fuel to determine the gas phase migration, the de- and adsorption of gases on the free surface of UO_2, and the lattice migration of Cs and I in LWR fuel. In order to determine de- and adsorption and the gas phase transport, they used I- and Cs-doped UO_2 powder, placed in a thermal gradient tube with a temperature of 200 °C at the tube end and between 1000-1400 °C in the center. I and Cs both concentrated in the colder regions, however, iodine was found to migrate slightly faster, contradicting excessive formation of CsI during redistribution. As UO_2 is known to act as catalyst for dihalogen splitting, the experiment was repeated with MgO. The results obtained were identical to the first experiment. Small leaks were introduced in the cold end of the heating device and they showed that iodine escaped completely and cesium remained in the device. The conclusion reached from this experiment was that desorption of cesium and iodine from the free surface of the UO_2, the gas phase migration, and the adsorption in the outermost cool region occurs very fast under simulated LWR fuel temperature conditions. Hence, a reaction to form CsI did not seem to have taken place [23]. When studying iodine and cesium migration in the bulk, it was found that iodine present in the lattice does not redistribute significantly up to 2000 °C. Similarly, it was found that an increase in the linear power up to 420 W/cm had little effect on the redistribution. Similar results were found for Cs. Above the threshold cesium and iodine were found to redistribute in the fuel like noble gases. This was confirmed by similar experiments by Sontheimer et al. [24], who also found that iodine and cesium did not redistribute significantly in axial direction of the fuel pin. In a later study by Peehs et al. [25], irradiated fuel samples with a burn-up of 33 GWd/tHM were investigated using a Knudsen cell and the results revealed that the release rate of iodine was slightly higher than that of Cs. The different release rates were taken as an indication of the different chemical state of the two elements.

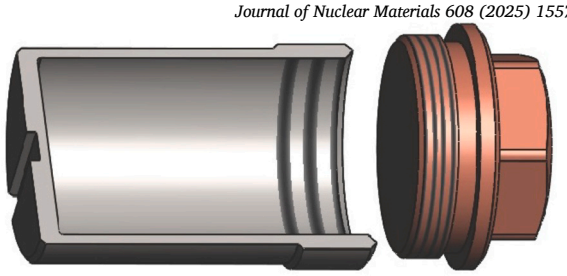

Fig. 1. Rendering of the stainless steel container (cut) with its copper lid.

In conclusion, the form of cesium and iodine in nuclear fuel is still disputed. Arguments such as thermodynamic stability and similar deposit characteristics of iodine and cesium lean towards the hypothesis that CsI is formed in nuclear fuel. However, arguments such as dissociation of CsI due to the radiation field and/or dissimilar diffusion rates contradict this hypothesis. In this paper, we aim finding conclusive arguments to support or disprove the formation of CsI in nuclear fuel by investigating the release of cesium and iodine from irradiated fuel samples using Knudsen effusion mass spectrometry, and comparing the results with pure CsI, as well as CsI-doped UO_2 simulated fuel.

2. Experimental

2.1. Samples

2.1.1. CsI

A single phase CsI sample was taken from powder purchased at Sigma Aldrich (Pure quality), which had a purity of 99.99%. The mass of the sample for the KEMS measurement was 15 mg. Prior to measurement, the CsI was dried at 300 °C for 3 hours under argon as halide salts are known for their moisture-absorbing properties. Its purity was verified by melting point determination, with no indication of impurities found.

Some CsI samples were also exposed to gamma irradiation. For this purpose the samples were enclosed in stainless steel containers with a copper lid (Fig. 1), in a second containment of aluminum that could be placed between spent nuclear fuel rods in the storage of the JRC hot cells in Karlsruhe. The duration of the "irradiation" was 427 days. Since the goal of the irradiation was to study the effects in a qualitative manner, it was not instrumented and only estimates for accumulated dose (10^5-10^6 Gy) and temperature (40-50 °C) can be provided.

2.1.2. UO_2+CsI

Two CsI-doped UO_2 simulated fuel samples (SPS1 and SPS2) were produced using spark plasma sintering (SPS), as described in more details elsewhere [26]. Briefly, a commercial UO_2 powder was mixed with 2.5 mol% CsI powder. The oxygen to uranium (O/U) ratio of the starting urania was determined by XRD as 2.10. This powder was used as-received for SPS1, and after annealing for 4 h in Ar/H_2 6.5% for SPS2. The samples were sintered in SPS with a ramp of 200 K/min up to 1273 K (SPS1) or 1423 K (SPS2) with 5 min dwell and a pressure of 70 MPa.

The as-produced samples had an O/U ratio of 2.03, a relative density of 99% and a grain size around 1.3 μm (SPS1), and O/U of 2.00, around 93-95% relative density (SPS2) and a grain size of 0.65 μm. A small fraction of the CsI evaporated during sintering, so that the given composition is the nominal one. The CsI inclusions were finely dispersed and mainly located at the grain boundaries at their triple junctions as confirmed by the SEM/EDX analysis shown in Fig. 2.

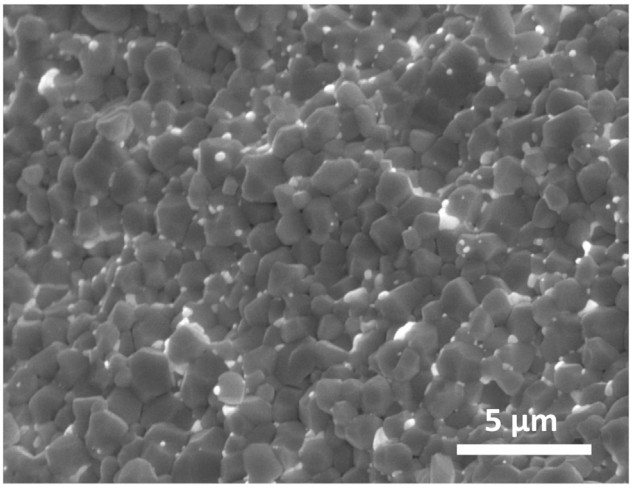

Fig. 2. Fracture surface of SPS1 sample (2.5 mol% CsI – UO_2). White spots are the CsI clusters at the grain boundaries.

2.1.3. Reactor irradiated fuel samples

The three irradiated UO_2 samples were taken from a commercial power plant rod. They were extracted from a long drill of a specific length of the fuel pin, and the radial position for each three samples was the same, the center of the pellet. The only significant difference between samples S1, S2 and S3 was the burn-up, 67 MWd/kgU for S1 and 55 MWd/kgU for S2 and S3, resulting from differences in axial positions. The irradiation temperature of the samples is estimated to be between 1400 and 1500 K which is according to [17,18] favorable for formation of CsI in the matrix. Within this burn-up range, the fuel may be slightly hyperstoichiometric. For experimental reasons, the S2 samples was measured with a 2 mm Knudsen effusion hole while the other ones with 0.5 mm hole. This may affect the release profile delaying Cs compared to iodine. This difference is difficult to assess experimentally because sample of such size may be different. However, we consider that given the time scale of the release period (10 K/min) the major driver is still the release kinetics. Each sample consisted of fragments with a size of around 100 µm and a total weight of few mg.

2.2. Experimental set-up (KEMS)

Cesium and iodine speciation of all samples were analyzed using a Knudsen effusion mass spectrometer (KEMS) that was built into an α-tight and lead-shielded glove-box to allow measurements on highly-radioactive material. The KEMS consists of a high temperature furnace with a small crucible (Knudsen cell) placed inside. The cell is coupled to a QMG422 quadruple mass spectrometer from Pfeiffer Vacuum GmbH.

The Knudsen cell itself is a small tungsten crucible of 21 mm in height and 11 mm in diameter. It consists of two parts, a sample holder and a removable lid. The lid has a small circular orifice of 0.5 mm (or 2 mm) in the middle, through which gaseous species can effuse. Normally, this orifice helps maintaining a molecular flow and ensuring an equilibrium between the condensed phase in the crucible and the effusing species. In this study, however, the fission product release is kinetically driven, so the diameter of the orifice does not play a significant role in the range of temperature of release measured.

Once the gaseous species effuse from the Knudsen cell they travel to an ionizing chamber, where they are bombarded with electrons and are converted to ionic species. The newly ionized species then travel further until they reach the mass spectrometer, where they are recorded according to mass. The masses recorded by the spectrometer range from 1 to 512 amu. For more details on the Knudsen cell method the reader is referred to [27].

In the case the KEMS is used for equilibrium studies, e.g. determining the vapor pressure of CsI, a known quantity of a reference material is vaporized simultaneously to obtain an experimental and unique calibration factor. In this study, Ag was the reference material of choice, as it has a well-known pressure and its gaseous species are inert toward the analyzed species.

By evaporating the reference material a calibration factor, K, is obtained. The calibration factor consists of two terms: (1) k_{Ag}, which is an instrumental term and independent of the sample, and (2) k_i, which is a term that is sample dependent. The calibration factor is described as:

$$K = k_{Ag} \times k_s \tag{1}$$

where k_{Ag} is defined as

$$k_{Ag} = \frac{P_{Ag}}{f_{Ag} \times I^+_{Ag} \times T_{Ag}} \tag{2}$$

P_{Ag} is the partial pressure of the silver, f_{Ag} is the fractional abundance of the Ag isotope considered, I^+_{Ag} is the intensity of the signals of the Ag isotopes, and T_{Ag} is the temperature. k_i is defined as follows:

$$k_i = \frac{f_i \times \sqrt{M_i} \times \sigma_{Ag}}{f_{Ag} \times \sqrt{M_{Ag}} \times \sigma_i} \tag{3}$$

where f_i is the isotope ratio of the species i, M_i is the molar mass of species i, M_{Ag} is the molar mass of silver, f_{Ag} the isotope ratio of Ag, σ_{Ag} is the ionization cross section of silver and σ_i is the cross section of species i. The square root of the mass of the isotope is commonly used as estimated yield of the SEM (secondary electron multiplier) when used in current mode.

Once the calibration factor is known, the vapor pressure of the species can be calculated. The vapor pressure of the species i is calculated according to Eq. (4), where, P_i is the partial pressure, I_i is the intensity of the signal, T is the temperature, and K the calibration factor as given in Eq. (1) [28].

$$P_i = I^+_i \times T_i \times K \tag{4}$$

It should be noted that the dissociation of the gaseous species into their ionized counterpart is not one-to-one. This means that e.g. CsI(g) upon being bombarded may be ionized to form CsI^+, but also to a certain fraction to Cs^+ or I^+, depending on the electron energy used. This fraction (of dissociation) can be determined by a so-called ionization efficiency measurement, performing an isothermal experiment in which the electron-energy is varied and the threshold energies and molecular yields are determined. Fig. 3 shows the ionization efficiency curves measured for pure CsI in this study. These fractions should be taken into account when calculating the pressure, as to not under- or overestimate it.

3. Fission product release from nuclear fuel

Gaseous and volatile fission products may affect the behavior of nuclear fuel in normal or abnormal operation [29]. The release profiles of fission gases and volatiles fission products during laboratory thermal treatments/anneals follow several steps that can be described by different mechanisms that include trapping/de-trapping from defects, diffusion, venting. The release can be observed as bursts or more continuous releases as shown, for example, in [3,30–32].

The release profiles of fission gases and volatiles typically show four characteristic release steps as a function of temperature, as depicted in Fig. 4, related to the microstructure and/or to the transport properties of the fuel and their change with temperature. After they are generated, the fission products may be trapped at voids or defects in the crystalline structure of the UO_2 matrix but also in larger sinks being grain boundaries or bubbles. The irradiation conditions like temperature and/or burn-up determine the onset and temperature ranges of the different observed release steps as well as their magnitude whereas the temperature during annealing determines the evolution of the microstructure

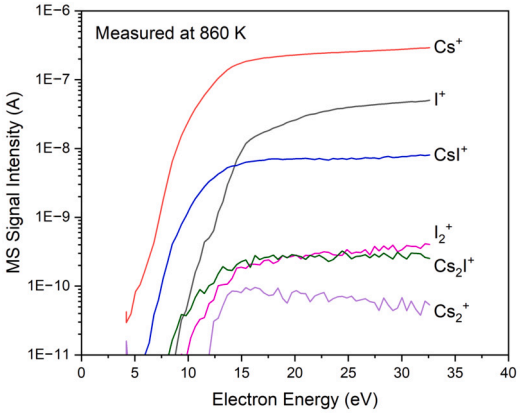

Fig. 3. The measured intensities at 860 K of the ionized species produced in the vapor of CsI as a function of the electron energy. The ionic fragments arise from two different species, CsI(g) and Cs_2I_2(g). (For interpretation of the colors in the figure(s), the reader is referred to the web version of this article.)

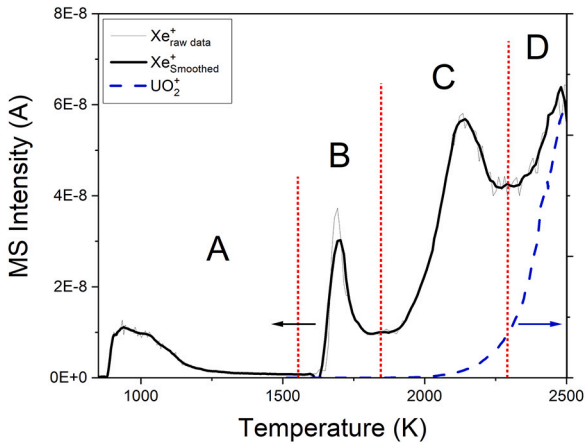

Fig. 4. Different release stages of Xe from S1 sample as measured by KEMS. From left to right the fission product releases are governed by the following processes: A, release of labile fraction from surfaces and cracks; B, atomic diffusion and grain boundary release; C, gas bubble growth and release; D, release of the residual fraction in the matrix.

and fission product behavior, eventually beyond the fuel operating conditions.

As an example, Fig. 4 shows the different stages of release of the inert fission gas Xe from the S1 sample as measured by Knudsen effusion mass spectrometry (KEMS). It is clearly seen from the graph that a first release (stage A) starts at approximately 800 K and ends before 1250 K. Some authors have also reported a minor release peak of fission gases at approximately 600 K (not present here) but this is irrelevant and possibly biased by experimental artifacts [33]. This first release we observe here is associated to diffusion via defects present from the irradiation.

The second release (stage B) is due to thermal diffusion through the matrix to the grain boundaries [34]. As mentioned above, radiation has created damage in the crystalline matrix in the form of vacancy clusters and dislocation loops, which act as trapping sites for fission products and cause retardation of release. The release is then a fraction of gas diffusing whereas it also competes with trapping at defects or in voids [35]. When the concentration of atoms at the trapping sites is high enough, gas-gas interactions occur which lead to the formation of fission gas bubbles [37].

During irradiation and in the presence of radiation, radiation-induced re-solution in the fuel matrix occurs [37]. When the fission products reach a grain boundary surface they aggregate in lenticular-shaped gas bubbles for example. As the concentration of the fission product bubbles at the grain boundary increase with time, the bubbles will grow and tunnels at the grain edges form through which they can be released to the free volume in the fuel pin [36].

The mobility of fission gas bubbles is controlled by the temperature gradient in the fuel pellet and the typical temperature for the start of fission gas bubble diffusion is between 1200 °C and 1600 °C for (near) stoichiometric UO_2 fuel, which is above the typical temperatures occurring in LWR fuel during normal operation. This is reflected during laboratory anneals in stage C in Fig. 4. Similar mechanisms were also observed for the migration of implanted cesium in UO_2 as described in by Panetier et al. [38].

The last of the four fission product release stages (D) in the mass spectrometric experiment (Fig. 4) starts once the matrix starts evaporating significantly, which occurs at relatively low temperature due to the specific conditions (small sample size, vacuum, experimental conditions; see below). Not all fission products find their way into a grain boundary or a fission gas bubble. Some fission products are incorporated into the crystal lattice of the fuel matrix and some are trapped at defect sites and in pores and are thus only released when the matrix start to evaporate. The point at which the matrix starts to evaporate in the KEMS experiments depends on the fuel stoichiometry. In the experimental condition of the current study, it can be as early as 1500 K for highly oxidized fuel or as late as 2000 K [2], as we see in our graph, for typical stoichiometric fuel.

4. Results

4.1. CsI

The first analyzed sample was pure CsI. The sample was then heated in the KEMS at a rate of 10 K/min until reaching 1100 K, at which point it was fully vaporized. To account for the dissociation of the CsI gaseous species at the electron energy used during the experiment (29.5 eV), an apparent potential curve was recorded at a constant temperature of 860 K. The obtained appearance potential curve is presented in Fig. 3. This figure differs somewhat from the similar plot in our previous study [7], where we observed an inflection shoulder at low energies of the Cs^+ signal. At that time, the shoulder was interpreted as a signal arising from Cs(g) atomic species. However, through a series of background and degassing experiments, it was determined that this initial increase in the Cs^+ signal is related to a memory effect rather than Cs(g) species in equilibrium with the CsI compound. Nevertheless, the quantity related to Cs(g) species in our previous paper was identified as negligible (less than 0.27 mol%), thus not negatively impacting the study's outcome. The partial vapor pressures of CsI(g) and Cs_2I_2(g) are in good agreement with the critically assessment reported in the NIST-JANAF tables [39].

Roki et al. [40] critically assessed the thermodynamic properties of CsI solid, liquid and gas phases. In their review, they analyzed the vaporization of CsI(s) based on the signals obtained for the dimer-to-monomer pressure ratio. For this they compared twelve individual studies. In all of them Cs^+, CsI^+, Cs_2I^+ were observed. In most studies also I^+ and in a few studies Cs_2^+ were observed. One study reported CsI trimers and tetramers. The ratios derived from Fig. 3 are (100:15.6:2.75) for (Cs^+:CsI^+:I^+) at 25 eV and 860 K. These numbers are in agreement with the range that Roki et al. [40] indicate in their assessment.

4.2. UO_2+CsI (SPS1 and SPS2)

Next, the CsI-doped UO_2 samples (SPS1 and SPS2) were analyzed to determine whether the vaporization of CsI is different when incorporated in a UO_2-matrix. The associated graphs are shown in Fig. 5.

The CsI release of SPS1 and SPS2 started at 800 K and 1100 K, respectively, which is consistent with the temperature at which grain boundary release takes place. The release temperatures are also consistent with Fig. 2, which showed that CsI accumulated at the grain boundaries of the UO_2 matrix.

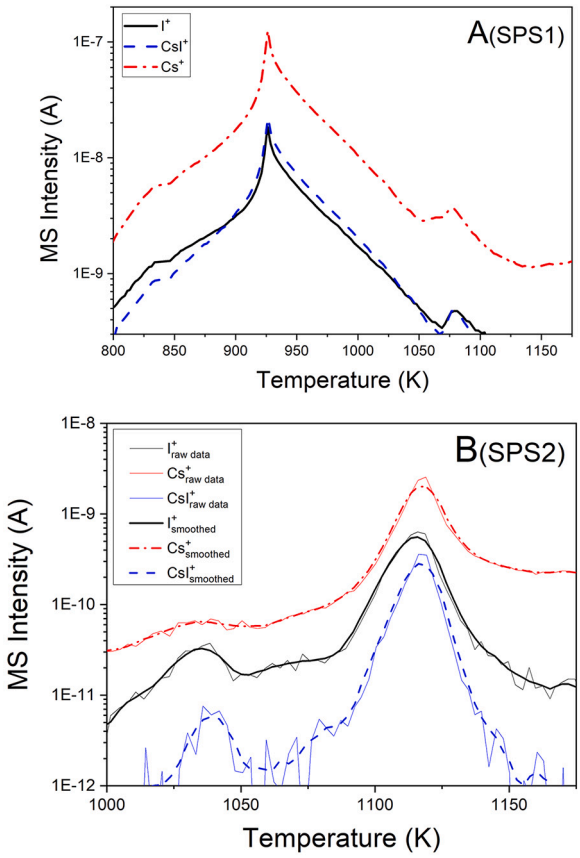

Fig. 5. The measured intensities of the Cs^+, I^+ and CsI^+ ionized species from UO_2+CsI samples SPS1 (A) and SPS2 (B) at T = 1100 K [7]. The thick lines show a smoothed curve of the experimental data.

The only signals observed in both SPS1(O/U = 2.03, 99% density) and SPS2(O/U = 2.00, 93-95% density) are signals Cs^+, I^+ and CsI^+, similar to pure CsI sample. Other signals such as I_2^+, $Cs_2{}^+$ and Cs_2I^+, were below the detection limit. The signals are reasonably parallel, which potentially indicates a congruent vaporization source.

The ratios of the signals of Cs^+, I^+ and CsI^+, in addition to be parallel, correspond relatively closely to the ones observed over pure CsI (Fig. 3 at 29 eV). However, the I^+ signal of SPS1 shows the particularity that the ratio I^+/CsI^+ is lower than expected, but this may be due to the sharp release as the masses are not measured at the same time and to the experimental uncertainty.

The earlier release for sample SPS1 can have several causes. It can be due to the extremely high density of SPS1 (99% relative density) which caused cracking and fracturing at lower temperature as opposed to the sample SPS2 (93-95% relative density). This favors the mobility of CsI at the grain boundaries. Another explanation could be the higher O/M ratio of SPS1 as a result of which the oxidized surface of the grains is more prompt to mobility of atoms [41], favoring the migration of CsI as well. This also explains the fact that the SPS sintering at 1273 K of $UO_{2.10}$ powder leads to an higher density sample (99%) than the sintering of $UO_{2.00}$ at 1423 K resulting to a density of 93-95%. Finally, it cannot be excluded that CsI reacted with the matrix to form Cs_2UO_4 due to the higher oxygen potential. We favor the first explanation as the release shows very sharp parallel curves for Cs and I.

Transposing these results to irradiated fuel under the assumption that (almost) all iodine is bound to Cs, implies that we should expect a similar ratio between I^+ and CsI^+ and the same release pattern of these signals. Their ratios to Cs^+ cannot be used in case of irradiated fuel, as Cs is produced in a 10 times larger yield compared to iodine, and potentially the intensity of its signal will be higher and the profile of the signal different.

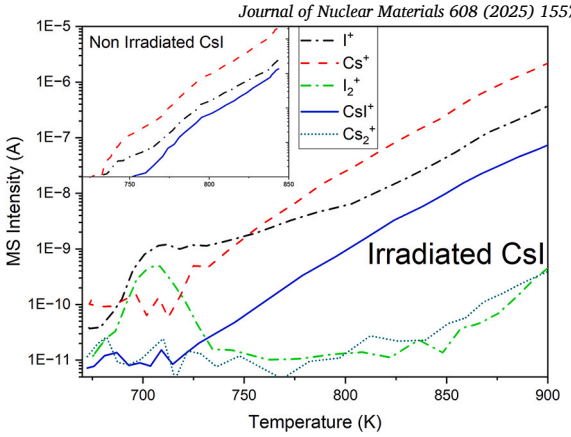

Fig. 6. The measured intensities of the Cs^+, I^+, I_2^+, Cs_2^+ and CsI^+ ionized species from the gamma-irradiated CsI sample and from pure CsI as comparison.

4.3. Gamma-irradiated CsI samples

After the gamma-irradiation a change in the color (toward light pink) of the white sample was observed. The KEMS experiment of the sample, performed 33 days after unloading, showed a change of the ionized species in the vapor compared to the CsI sample, as can be seen in Fig. 6. First, we observed significant signals of I^+ and I_2^+ at the start of the experiment, with a maximum at about 700 K. No cesium release was observed in this temperature range. Above 725 K also the signals of Cs^+, CsI^+ and Cs_2^+ appeared, whose intensity ratios are similar to pure CsI. An important additional observation is that after the experiment, the background signal for I_2^+ remains high, indicating a memory effect, i.e. condensation of I_2 on the mass spectrometer head, and a thorough cleaning of the mass spectrometer was needed to achieve the original background values. These points towards the presence of a compound which is highly volatile in the sample, likely elemental iodine.

We thus conclude that the CsI sample partially decomposed during the gamma irradiation with dose rate typical for spent fuel, forming elemental iodine and cesium. Also elemental cesium is volatile, but since the sample was handled in a nitrogen atmosphere with some oxygen as impurity, its oxidation will undoubtedly have occurred, and is therefore not detected at low temperature. For that reason back reaction to CsI during heating will have been limited.

4.4. Reactor-irradiated fuel samples

4.4.1. S1 sample

As shown in Fig. 7, no CsI^+ signal was observed for sample S1 over the entire temperature range. For Cs^+ and I^+, however, we did observe a signal with two release peaks in the studied temperature range. The first and smallest peak centers around 975 K (signal starts around 800 K and disappears around 1200 K) and can be associated with grain boundary release. This is consistent with the release earlier observed in the SPS-samples.

For the second release peak the signal for I^+ starts at 1700 K and ends at 2000 K, whereas the signal for Cs^+ starts at 1700 K but only disappears after 2300 K. The signals for I^+ and Cs^+ follow a different trend indicating that they do not stem from the same compound, CsI. There is a partial overlap of the release of both species that could indicate a common CsI source which is not confirmed by the presence of the CsI^+ signal The I^+ signal has a relatively sharp width whereas the Cs^+ peak has a broader width and more gradual evolution, indicating that the release processes for the two elements are different.

A remark should be made about which atomic masses were used to construct the Cs^+, I^+ and CsI^+ curves for the irradiated fuel. The Cs^+ signal is the sum of the atomic masses 133, 135, and 137. Similarly, for the I^+ signal the intensities of atomic masses 127 and 129 were taken

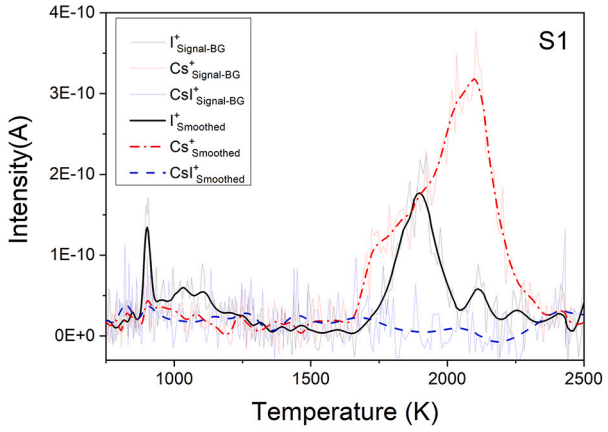

Fig. 7. The measured intensities of the Cs^+, I^+ and CsI^+ ionized species from the S1 sample. The thick lines show a smoothed curve of the experimental data.

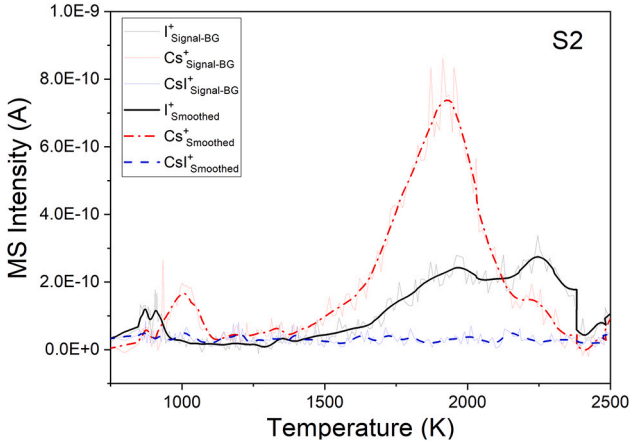

Fig. 8. The measured intensities of the Cs^+, I^+ and CsI^+ ionized species from the S2 sample. The thick lines show a smoothed curve of the experimental data.

and the CsI^+ curve consists of signals obtained for atomic masses 260, 262, 264 and 266. Some of the double ionized actinide oxides interfere in the spectrum with some of those masses, especially above 2300 K. The signals shown in the figures have been corrected for this interference by subtracting a constant fraction of the single ionized signal to the signal at the mass of the double ionized. The fraction factor was determined in order to remove the obvious interference.

4.4.2. S2 sample

Similar to S1, we observed signals for Cs^+ and I^+ but not for CsI^+, and two release peaks. However, some aspects of the release curves for sample S2 are partly different (Fig. 8):

- The intensity of the first release is significantly higher than in S1, suggesting a larger fraction of these fission products in the grain boundaries.
- The initial release peaks for I^+ and Cs^+ coincide, but we observe an immediate increase for Cs^+ after, and not for I^+. This pattern was more pronounced, but not fully different from S1, in which this release stage was smoother.
- Whereas the second release peaks for I^+ and Cs^+ in sample S1 were markedly different, the peaks of I^+ and Cs^+ in sample S2 were very similar.

4.4.3. S3 sample

The results for sample S3 (Fig. 9) indicate a very small Cs^+ release around 1000 K, the grain boundary release stage. A large second peak

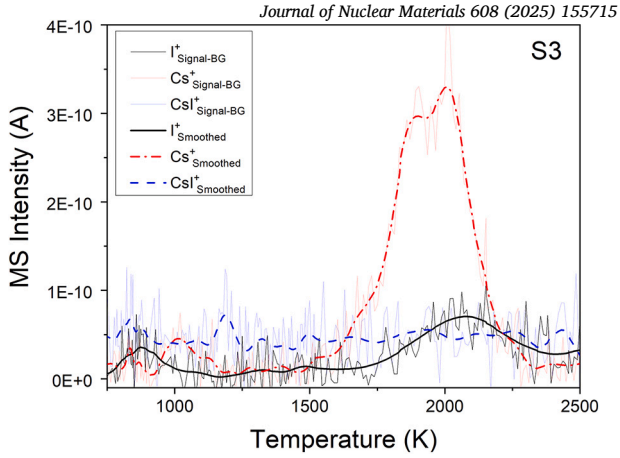

Fig. 9. The measured intensities of the Cs^+, I^+ and CsI^+ ionized species from the S3 sample. The thick lines show a smoothed curve of the experimental data.

was observed for Cs^+, which can be assigned to release resulting from matrix diffusion. The peak started at 1600 K and ended at 2250 K and the I^+ release was small compared to Cs^+, and thus different from S1 and S2.

5. Discussion

The experiments performed with the CsI and SPS-samples lead to the following requirements for confirmation of the presence of CsI in UO_2 nuclear fuel: (i) The mass spectrometric curves should reveal both Cs^+, I^+ and CsI^+ signals, (ii) the signals for I^+ and CsI^+ must behave identically, and (iii) the ratio between the two signals should be at lowest 1:0.7. Based on these results, we will now first discuss the observations for the three main temperature ranges, representing grain boundary release, followed by matrix diffusion and finally matrix evaporation.

- For the irradiated samples S1 to S3, I^+ and Cs^+ peaks were observed in the temperature range of 800 K to 1200 K and can be assigned to grain boundary release. The curves partially matched in shape, which could indicate that they may stem from the same compound. However, no signal for CsI was observed. Based on the I^+:CsI^+ ratio found in the SPS-samples (1 to 0.7), the CsI^+ signals should have been detected for samples S1 and S2.
- Cs^+ and I^+ peaks were observed in the 1500 K to 2250 K temperature range and again no CsI^+ signal was observed. In sample S1, the Cs^+ and I^+ curve were markedly different. The I^+ signal had a smaller width than the Cs^+ signal, whereas the Cs^+ signal, indicating different diffusion and release mechanisms. The Cs^+ and I^+ signals of S2 and S3 did exhibit parallel release curves, indicating that they could have the same origin. However, when the signals are compared to the signal of fission gases as shown in Fig. 1, we see that all fission gasses and volatiles have similar release behavior starting at 1500 K (matrix diffusion) indicating similar diffusion characteristics and not a similar chemical origin.
- Above 2250 K no ionic Cs^+ and I^- species were observed.

Thus, none of the samples met the requirements to confirm the presence/formation of CsI in nuclear fuel. The CsI^+ ionized species was detected in neither of the three samples S1, S2 and S3 and the correct peak ratio between I^+ and CsI^+ was not fulfilled. However, we did observe similar release behavior of I^+ and Cs^+. In all three samples, we observed release up to 1000 K for the two elements and we observed a major release starting at 1500 K. The similar release behavior is caused by both elements being present in their volatile form as explained earlier on. The differences in the release patterns of the first and second stages between the S1, S2 and S3 samples may be attributed to differ-

ences in the axial positions, but also to stochastic differences inherent to complicated experiments with small-sized nuclear fuel samples.

The absence of CsI in our experiments can have two reasons: (i) It was not formed during reactor operation. (ii) It was no longer present in the fuel at the moment of the experiments. We will shortly discuss the two possibilities.

As discussed in the introductory sections, numerous experimental observations have been published and arguments presented on the formation of CsI in nuclear reactor fuel, with inconclusive results. Additional arguments may come from theoretical pair potential calculations by Grimes et al. [42]. They showed that in UO_2 fuel the site preference of an I ion is a di-oxygen vacancy and the site preference of Cs is a uranium vacancy, or Cs_2 in a tetra-vacancy. As specific defects tend to cluster it is possible that in the fuel matrix Cs and I migrate along different paths with a limited probability of meeting each other. However, if they do meet the clustering of Cs and I would be favorable by 0.43 eV at a charged tetra-vacancy in UO_2 compared to separate ions [42]. Also when reaching the grain boundaries they might react (e.g. Cs + I → CsI), depending on the surface concentration of the fission products. The rate of desorption of individual fission products (e.g. Cs and I) is proportional to their surface concentration, which in turn is directly related to the burn-up. This means that the rate of formation of a compound (CsI) is approximately proportional to the square sum of the burn-up [43]. So when the burn-up is high it is more likely that fission product compound desorbs from the surface, whereas when the burn-up is low (e.g. trace-irradiated UO_2) the desorption of elemental fission product is favored. Our results for a relatively high burn-up indicate that Cs and I are not released as molecular CsI.

Therefore we must take into account the fact that it is highly probable that CsI decomposes in a gamma radiation field [22,44,9,45]. In view of the long storage time (8 year) it is thus well possible that in-reactor formed CsI is no longer present at the time of the mass spectrometric measurement. As discussed, Cubiccioti et al. [22] found evidence that CsI dissociates in a gamma radiation field at dose of a 10^6-10^7 Gy and temperatures of 320 K, 443 K, and 570 K in vacuum. Kulikov and Malyshev [44] found similar results at a dose of 10^4-10^6 Gy and temperatures of 318 K and 623 K in air. They analyzed the decomposition products in the solid and gaseous phase and found that a significant fraction (> 50%) of iodine remained in the powder. They also found no strong dependence of the dose rate (from 0.3 to 20 Gy/s), whereas the yield was twice as high at 318 K compared to 623 K. Bibilashvili et al. [9] investigated the effects of temperature and helium pressure on the radiolytic decomposition of CsI, and concluded that with increase of both the decomposition increases. The temperature dependence is different from the earlier observations, but is due to the specific experimental setup in which an increasing amount of gaseous CsI was exposed with increasing temperature. Thus, all three studies provide strong evidence that gamma radiation during the storage period of the samples studied may have resulted in an almost complete destruction of CsI, if it was present.

Our KEMS experiments with gamma-irradiated CsI confirm the effect of radiolytic decomposition of CsI, at similar dose and a dose rate typical for spent nuclear fuel. The obtained results were qualitative, so it is difficult to assess the exact impact of years of storage of the nuclear fuel on the chemical speciation of the fission products, and especially Cs and I. But considering all evidence from this study and literature, we conclude that formation of CsI in nuclear fuel at grain boundary is likely, but it is decomposed by strong and continuous gamma radiation in reactor but particularly during post-irradiation storage at low(er) temperature, making it impossible to detect CsI in the analyzed fuel samples.

It is interesting to note that in earlier mass spectrometric studies of irradiated fuel we did find evidence for CsI formation and release [31,3]. In that work we studied the fission gas release from oxidised irradiated fuel, and the CsI^+ ion was observed in the release curves of a pre-oxidised sample, i.e. after a heat treatment in air at 670 K, which resulted in a composition close to U_3O_8. The intensity of the CsI^+ signal was about 0.1 of the I^+ signal, significantly lower than the one from the SPS samples, and the release took place in a broad release between 750 and 1750 K. Evidently, the thermal treatment and the oxidation gave Cs and I the opportunity to partially recombine at the grain boundaries and the gamma dose was low enough not to completely decompose the formed CsI.

6. Conclusion

Overall, no conclusive evidence was found for CsI release from irradiated fuel samples of burn-up of 55-65 MWd/tHM after several years of storage. The observation that this is different from fuel that was thermally treated at low temperature and oxidised before the measurement, is an indication that the reaction between Cs and I does easily take place. We must therefore conclude that radiolytic decomposition may have prevented CsI formation or decomposed the formed CsI during the long storage at low temperature.

CRediT authorship contribution statement

J.-Y. Colle: Writing – review & editing, Investigation, Formal analysis. **J.N. Zappey:** Writing – original draft, Investigation, Conceptualization. **O. Beneš:** Writing – review & editing, Investigation, Formal analysis, Conceptualization. **M. Cologna:** Writing – review & editing, Investigation. **T. Wiss:** Writing – review & editing. **R.J.M. Konings:** Writing – review & editing, Writing – original draft, Conceptualization.

Declaration of competing interest

The authors declare that they have no known competing financial interests or personal relationships that could have appeared to influence the work reported in this paper.

Acknowledgements

The authors wish to acknowledge the assistance of Tadeas Wangle and Vaclav Tyrpekl for the SPS sample fabrication, Gerard Montagnier and Abdelilah El-Abjani for help with the gamma irradiation, and Bert Cremer for SEM analysis.

Data availability

Data will be made available on request.

References

[1] E.H.P. Cordfunke, R.J.M. Konings, J. Nucl. Mater. 152 (1988) 301–309.
[2] R.J.M. Konings, O. Beneš, T. Wiss, Nat. Mater. 14 (2015) 247–251.
[3] J.Y. Colle, T. Wiss, O. Dieste, P. Pöml, D. Staicu, T. Tverberg, S. Brémier, R.J.M. Konings, V.V. Rondinella, T. Sonoda, A. Sasahara, S. Kitajima, J. Nucl. Mater. 578 (2023) 154340.
[4] C. Ronchi, M. Sheindlin, D. Staicu, M. Kinoshita, J. Nucl. Mater. 327 (2004) 58–76.
[5] R.J.M. Konings, T. Wiss, C. Guéneau, Chapter 34, L. R. Morss and N. Edelstein and J. Fuger and J. J. Katz, (Ed.) Springer Verlag, 2010, pp. 2113–2224.
[6] H. Kleykamp, J. Nucl. Mater. 131 (1985) 221–246.
[7] O. Beneš, E. Capelli, N. Vozárová, J.Y. Colle, A. Tosolin, T. Wiss, B. Cremer, R.J.M. Konings, Phys. Chem. Chem. Phys. 23 (2021) 9312.
[8] S. Shann, D. Olander, J. Nucl. Mater. 113 (1983) 234–248.
[9] Yu.K. Bibilashvili, M.V. Vladimirova, I.S. Golovnin, I.A. Kulikov, V.V. Novikov, A.S. Sotnikov, At. Energy 61 (1985) 93–95.
[10] P.S. Sidky, J. Nucl. Mater. 256 (1998) 1–17.
[11] R. Pulham, M. Richards, J. Nucl. Mater. 187 (1992) 39–42.
[12] D.C. Fee, C.E. Johnson, J. Nucl. Mater. 96 (1981) 71–79.
[13] K. Kadyrzhanov, J. Lambert, Safety Related Issues of Spent Fuel Storage, Springer, 2007.
[14] R. Viswanathan, J. Nucl. Mater. 444 (2014) 101–111.
[15] F.G. Di Lemma, J.Y. Colle, O. Beneš, R.J.M. Konings, J. Nucl. Mater. 465 (2023) 499.
[16] T.M. Besmann, T.R. Lindemer, Nucl. Technol. 40 (1978) 297–306.
[17] O. Götzmann, J. Nucl. Mater. 107 (1982) 185–195.
[18] M. Rochedy, V. Klosek, C. Riglet-Martial, C. Onofri-Marroncle, D. Drouan, D. Reyes, P. Bienvenu, I. Roure, M. Cabié, L. Amamidani, J. Léchelle, M.A. Pinault-Thaury, J. Nucl. Mater. 581 (2021) 154450.

[19] D. Campbell, A. Malinauskas, W. Stratton, Nucl. Technol. 53 (1981) 111–119.
[20] J.L. Collins, M.F. Osborne, R.A. Lorenz, A.P. Malinauskas, Nucl. Technol. 81 (1988) 78–94.
[21] J. Davies, R. Boyle, J. Hanus, General Electric, Technical Report GEAP-51004, 1966.
[22] D. Cubicciotti, J.H. Davies, Nucl. Sci. Eng. 60 (1976) 314–319.
[23] M. Peehs, R. Manzel, W. Schweighofer, W. Haas, E. Haas, R. Würtz, J. Nucl. Mater. 97 (1981) 157–164.
[24] F. Sontheimer, W. Vogl, I. Ruyter, J. Markgraf, J. Nucl. Mater. 88 (1980) 131–137.
[25] M. Peehs, G. Kaspar, K.H. Neeb, J. Nucl. Mater. 119 (1983) 284–290.
[26] T. Wangle, V. Tyrpekl, M. Cologna, J. Somers, J. Nucl. Mater. 466 (2015) 150–153.
[27] M. Miller, K. Armatys, Open Thermodyn. J. 7 (2013) 2–9.
[28] J. Drowart, C. Chatillon, J. Hastie, D. Bonnel, Pure Appl. Chem. 77 (2005) 683–737.
[29] J. Rest, M.W.D. Cooper, J. Spino, J.A. Turnbull, P. Van Uffelen, C.T. Walker, J. Nucl. Mater. 513 (2019) 310–345.
[30] J.-Y. Colle, J.P. Hiernaut, T. Wiss, O. Beneš, H. Thiele, D. Papaioannou, V.V. Rondinella, A. Sasahara, T. Sonoda, R.J.M. Konings, J. Nucl. Mater. 442 (2013) 330–340.
[31] J.P. Hiernaut, T. Wiss, J.-Y. Colle, H. Thiele, C.T. Walker, W. Goll, R.J.M. Konings, J. Nucl. Mater. 377 (2008) 313–324.
[32] T. Wiss, J.P. Hiernaut, J.-Y. Colle, H. Thiele, V.V. Rondinella, R.J.M. Konings, A. Sasahara, T. Sonoda, Trans. Am. Nucl. Soc. 104 (2011) 285–286.
[33] Y. Pontillon, D. Parrat, S. Ravel, in: Proceeding 2004 International Meeting on LWR Fuel Performance, 2004, pp. 490–499.
[34] M. Hirai, J.H. Davies, R. Williamson, J. Nucl. Mater. 226 (1995) 238–251.
[35] H. Matzke, Radiat. Eff. 75 (1983) 317–325.
[36] M. Tucker, Radiat. Eff. 53 (1980) 251–255.
[37] H. Matzke, Radiat. Eff. 53 (1980) 219–242.
[38] C. Panetier, Y. Pipon, C. Gaillard, D. Mangin, J. Amodeo, J. Morthomas, T. Wiss, A. Benedetti, R. Ducher, R. Dubourg, N. Moncoffre, J. Chem. Phys. 156 (2021) 044705.
[39] M.W. Chase, J. Phys. Chem. Ref. Data, Monogr. 9 (1998).
[40] F.Z. Roki, M.N. Ohnet, S. Fillet, C. Chatillon, I. Nutta, J. Chem. Thermodyn. 70 (2014) 46–72.
[41] E. Moore, C. Guéneau, J.-P. Crocombette, J. Solid State Chem. 203 (2013) 145–153.
[42] R.W. Grimes, R.G.J. Ball, C.R.A. Catlow, J. Phys. Chem. Solids 53 (1992) 475–484.
[43] S.G. Prussin, D.R. Olander, W.K. Lau, L. Hansson, J. Nucl. Mater. 54 (1988) 25–37.
[44] I.A. Kulikov, M.L. Malyshev, At. Energy 55 (1983) 316–318.
[45] K. Konashi, Y. Shiokawa, H. Kayano, J. Nucl. Mater. 55 (1996) 181–185.